**Volume Title**
ASP Conference Series, Vol. **Volume Number**
**Author**




# [CII] 158$\mu$m Emission from $z \geq 10$ Galaxies

C. L. Carilli,[1,2] E.J. Murphy,[3] A. Ferrara,[4] and P. Dayal[5]

[1]*National Radio Astronomy Observatory, Socorro, NM 87801;* ccarilli@nrao.edu

[2]*Cavendish Astrophysics, Cambridge, UK*

[3]*National Radio Astronomy Observatory, Charlottesville, VA 22903;* emurphy@nrao.edu

[4]*Scuola Normale Superiore, Piazza dei Cavalieri 7, I-56126 Pisa, Italy*

[5]*Kapteyn Astronomical Institute, University of Groningen, P.O. Box 800, 9700 AV Groningen, The Netherlands*

**Abstract.** We consider the capabilities of ALMA and the ngVLA to detect and image the [CII] 158 $\mu$m line from galaxies into the cosmic 'dark ages' ($z \sim 10$ to 20). The [CII] line may prove to be a powerful tool in determining spectroscopic redshifts, and galaxy dynamics, for the first galaxies. In 40 hr, ALMA has the sensitivity to detect the integrated [CII] line emission from a moderate metallicity, active star-forming galaxy [$Z_A = 0.2\,Z_\odot$; star formation rate (SFR) = 5 $M_\odot$ yr$^{-1}$], at $z = 10$ at a significance of 6$\sigma$. The ngVLA will detect the integrated [CII] line emission from a Milky-Way like star formation rate galaxy ($Z_A = 0.2\,Z_\odot$, SFR = 1 $M_\odot$ yr$^{-1}$), at $z = 15$ at a significance of 6$\sigma$. Imaging simulations show that the ngVLA can determine rotation dynamics for active star-forming galaxies at $z \sim 15$, if they exist. The [CII] detection rate in blind surveys will be slow (of order unity per 40 hr pointing).[1]

## 1. Introduction

The $z \sim 15$ Universe is at the edge of our current understanding. A handful of theoretical studies have speculated on the cosmic star formation rate (SFR) density at these redshifts (Mashian et al. 2016; Duffy et al. 2017; Chary & Pope 2010; Dayal et al. 2014; Yue et al. 2015; Topping & Shull 2015). Observational constraints on extreme redshift galaxies are poor, based on extrapolation of the few galaxies and AGN known at $z \sim 7$ to 8, and the even fewer galaxy candidates at $z \sim 8$ to 11.

Encouraging results come from observations of a relatively mature interstellar medium, and active star formation, in some of the very high redshift sources discovered to date. The last few years have seen an explosion in the number of [CII] 158$\mu$m detections at high redshift, including high resolution imaging of the gas dynamics on kpc-scales in both AGN host galaxies and in more normal star-forming galaxies at

[1]This paper is a brief synopsis of a paper presented in the Astrophysical Journal (Carilli et al. 2017). We refer the interested reader to the Journal article for more detail.

$z \sim 5.5$ to 7.5 (see Carilli et al. 2017) for a summary). The most recent results include the detection of the [OIII] 88$\mu$m fine structure line and/or the [CII] line, from galaxies at $z = 7.2$, 8.4, and 9.1 (Laporte et al. 2017; Hashimoto et al. 2018a,b) and the detection of strong [CII] and dust continuum emission from a quasar host galaxy at $z = 7.5$ (Venemans et al. 2017). While encouraging, observations remain sparse, and the most basic questions remain on the nature, and even existence, of galaxies at $z \sim 15$.

Given the uncertainty in our knowledge of galaxies at extreme redshifts, in this study we focus on a few simple of questions: if such extreme redshift galaxies exist, what kind of facility is required to detect, and possibly image, the [CII] 158 $\mu$m line emission? How do the prospects depend on basic galaxy properties, such as metallicity and star formation rate? And based on what little we know of galaxy demographics at very early epochs, what kind of numbers can we expect in blind cosmological spectral deep fields?

## 2. The [CII] 158$\mu$m line

The [CII] 158 $\mu$m line is one of the brightest spectral line from star-forming galaxies at far-infrared wavelengths and longer, carrying between 0.1% to 1% of the total far infrared luminosity of star forming galaxies (Stacey et al. 1991; Carilli & Walter 2013). The [CII] fine structure line traces both neutral and ionized gas in galaxies, and is the dominant coolant of star-forming gas in galaxies (Velusamy et al. 2015). While the line is only visible from space in the nearby Universe, it becomes easier to observe with increasing redshift, moving into the most sensitive bands of large ground based millimeter telescopes, such as NOEMA[2], and the ALMA[3].

As a predictor for the [CII] 158 $\mu$m luminosity from early galaxies we use the Vallini et al. (2015) relationship (their Equation 8). This theoretical and observational analysis considers in detail the relationships between star formation rate, galaxy metallicity, and [CII] luminosity. We adopt a few representative galaxy characteristics, including the main parameters of star formation rate, metallicity, redshift, and [CII] luminosity, and compare these to the capabilities of the given facilities.

## 3. Telescopes

The relevant ALMA bands are 3, 4, and 5, corresponding to frequencies of 84 – 116 GHz, 125 – 163 GHz, and 163 – 211 GHz, respectively. These bands then cover the [CII] line (1900.54 GHz rest frequency), between $z = 10$ and 20, almost continuously, with gaps of a few MHz due to atmospheric $O_2$ absorption at 118 GHz and 183 GHz. The current bandwidth for ALMA is 8 GHz, with a upgrade to 16 GHz or 32 GHz being considered sometime in the future. We employ the ALMA sensitivity calculator, under good weather conditions (3rd octile), with 50 antennas. For the sake of illustration, we adopt a fiducial line width of 100 km s$^{-1}$ (see below) and an on-source integration time of 40 hr. The rms sensitivity per channel is 21 $\mu$Jy beam$^{-1}$ channel$^{-1}$, roughly

[2] http://iram-institute.org/EN/noema-project.php

[3] http://www.almaobservatory.org

independent of frequency due to the increasing channel width in Hz for a fixed velocity resolution, offsetting decreasing system sensitivity with increasing frequency.

Table 1. Facilities

| Telescope | Redshifts | Frequencies (GHz) | rms ($\mu$Jy beam$^{-1}$) | Bandwidth (GHz) |
|---|---|---|---|---|
| ngVLA | 15 – 20 | 116 – 90 | 2.0 | 26 |
| ALMA | 10 – 15 | 173 – 116 | 21 | 8 (32) |

For the ngVLA we employ the "Southwest" configuration, and we adopt sensitivity parameters consistent with ngVLA memo 17 (Selina & Murphy 2017). The maximum redshift we consider is $z = 20$, so we only consider frequencies between 90 and 116 GHz. The current reference design has a nominal maximum bandwidth of 20 GHz, although broader bandwidths are under investigation. For the sake of number counts, the $z = 18.8$ to 20 range (90 GHz to 96 GHz), contributes very little to the total number of sources detected in blind searches. For the purpose of estimating the sensitivity of the ngVLA for realistic observations, and to explore the imaging capabilities in the event of the discovery of any relatively luminous sources, we have employed the CASA simulation tools (Carilli & Shao 2017), developed for the ngVLA project.

We simulate a 40 hr observation, and we employ the CLEAN algorithm with Briggs weighting. We adjust the ROBUST parameter, the $(u, v)$-taper, and the cell size, to give a reasonable synthesized beam and noise performance. Our target resolution is $\sim 0\farcs4$ for detection, and $\sim 0\farcs2$ for imaging.

We adopt as a spatial and dynamical template, the observed CO 1-0 emission from the nearby star-forming disk galaxy, M 51 (Helfer et al. 2003). We arbitrarily reduce the physical size of the disk by a factor three, with the idea that very early galaxies are likely smaller than nearby galaxies. Again, this exercise is for illustrative purposes, and the input model is just a representative spatial/dynamical template for a disk galaxy, with the relevant parameters being size, velocity, and luminosity. We then adjust the line luminosity per channel per beam, to achieve a given integrated [CII] 158 $\mu$m luminosity at a given redshift.

## 4. Results

### 4.1. Spectroscopic Confirmation of $z \gtrsim 10$ Candidates

An obvious application of the [CII] 158 $\mu$m line search will be to determine spectroscopic redshifts for near-IR dropout candidate galaxies at $z \sim 10$ to 20. We start with the relationship between the [CII] velocity integrated line flux, in the standard flux units of Jy km s$^{-1}$, versus redshift. We adopt a metallically of $Z_A = 0.2\,Z_\odot$, and star formation rates of $1\,M_\odot\,\mathrm{yr}^{-1}$ and $5\,M_\odot\,\mathrm{yr}^{-1}$. Figure 1 shows the predicted [CII] line flux versus redshift for the two models, along with the $1\sigma$ sensitivity of ALMA and the ngVLA.

This image simulation shows that, in 40 hr, the ngVLA will be able to detect the integrated [CII] line emission from moderate metallicity and star formation rate galaxies ($Z_A = 0.2$, SFR $= 1\,M_\odot\,\mathrm{yr}^{-1}$), at $z = 15$ at a significance of $6\sigma$. This significance reduces to $4\sigma$ at $z = 20$.

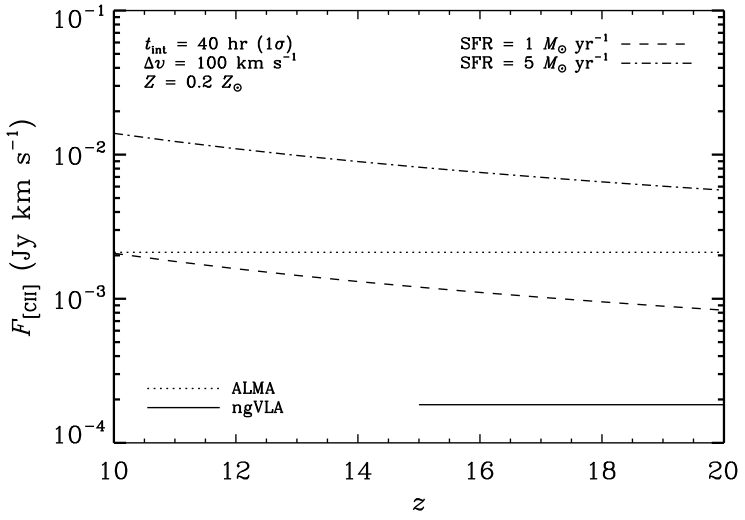


Figure 1. [CII] 158 $\mu$m velocity integrated line flux versus redshift for galaxies with star formation rates of 1 $M_\odot$ yr$^{-1}$ and 5 $M_\odot$ yr$^{-1}$, and metallicity of 0.2 $Z_\odot$, based on the relationship given in Equation 12 of Vallini et al. (2015). The rms sensitivity in a 100 km s$^{-1}$ channel and 40 hr integration is shown for both ALMA and the ngVLA.

In 40 hr, ALMA will be able to detect the integrated [CII] line emission from a higher star formation rate galaxy ($Z_A$ = 0.2 $Z_\odot$, SFR = 5 $M_\odot$ yr$^{-1}$), at $z$ = 10 at a significance of 6$\sigma$. This significance reduces to 4$\sigma$ at $z$ = 15. ALMA will be hard-pressed to detect a moderate metallicity ($Z_A$ = 0.2 $Z_\odot$), lower star formation rate (1 $M_\odot$ yr$^{-1}$) galaxy, requiring 1000 hr for a 5$\sigma$ detection of the velocity integrated line flux, even at $z$ = 10.

We next consider dependence on metallicity. Figure 3 shows the relationship between [CII] luminosity (in Solar units), to star formation rate, for three different metallicities: $Z_A$ = 0.04, 0.2, and 1.0 $Z_\odot$, for a galaxy at $z$ = 15. Again shown are the ALMA and ngVLA sensitivities in 40 hr, 100 km s$^{-1}$ channels. The Vallini et al. (2015) model has the [CII] luminosity as a strong function of metallicity. If the gas has Solar metallicity, the ALMA detection threshold (4$\sigma$) reduces to a galaxy with a star formation rate of 2.5 $M_\odot$ yr$^{-1}$ (compared to 5 $M_\odot$ yr$^{-1}$ for $Z_A$ = 0.2), while that for the ngVLA reduces to 0.4 $M_\odot$ yr$^{-1}$ (compared to 1 $M_\odot$ yr$^{-1}$ for $Z_A$ = 0.2). Conversely, for a low metallicity galaxy of $Z_A$ = 0.04 $Z_\odot$, these values increase to 100 $M_\odot$ yr$^{-1}$ and 10 $M_\odot$ yr$^{-1}$, respectively.

### 4.2. Kinematics of $z \gtrsim 10$ Galaxies

We investigate the potential for obtaining kinematic information from such galaxies using the ngVLA. We find that the best even the ngVLA can do for a $z$ = 15, $Z_A$ = 0.2 $Z_\odot$, and SFR = 1 $M_\odot$ yr$^{-1}$ galaxy, in 40 hr is a 5.5$\sigma$ detection of the integrated emission, with little or no dynamical information.

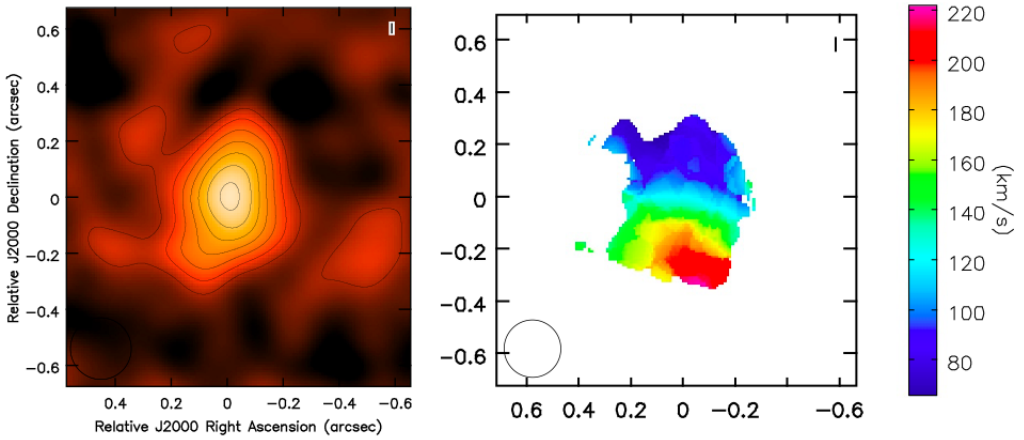


Figure 2. (*Left:*) A simulated image of the velocity integrated [CII] 158 $\mu$m emission from a $z = 15$ galaxy with a star formation rate of 5 $M_\odot$ yr$^{-1}$, and a metallicity of 0.2 $Z_\odot$, assuming for a 40 hr observation with the ngVLA. The contour levels are -6, -3, 3, 6, 9, 12, 15, 18, 21 $\mu$Jy beam$^{-1}$. The rms noise on the image is about 1.8 $\mu$Jy beam$^{-1}$, and the synthesized beam FWHM is 0.″22. (*Right:*) The intensity weighted mean [CII] velocity (moment 1).

For a higher SFR galaxy ($z = 15$, $Z_A = 0.2\,Z_\odot$, 5 $M_\odot$ yr$^{-1}$ galaxy), in a 40 hr observation, the ngVLA can recover the overall rotational dynamics of the system. The imaging results for the velocity integrated emission (mom 0), and the intensity weighted mean velocity (mom 1), are shown in Figure 2. The beam size in this case is FWHM $\sim$ 0.″2, and the channel images at 20 km s$^{-1}$ channel$^{-1}$ have an rms noise of 4.5 $\mu$Jy beam$^{-1}$.

### 4.3. The Potential for Blind Searches of $z \gtrsim 10$ Galaxies

Another application for the [CII] line will be blind cosmological deep fields. The advent of very wide bandwidth spectrometers has led to a new type of cosmological deep field, namely, spectral volumetric deep fields, in which a three dimensional search for spectral lines can be made, with redshift as the third dimension (Walter et al. 2016).

Table 2. Number of Detections per 40 hr Pointing

| Model | ngVLA $15 < z < 16$ | ngVLA $15 < z < 20$ | ALMA $10 < z < 10.5$ (8 GHz) | ALMA $11 < z < 14$ (32 GHz) |
|---|---|---|---|---|
| CP10, 1 $M_\odot$ yr$^{-1}$ | 0.29 | 1.3 | – | – |
| CP10, 5 $M_\odot$ yr$^{-1}$ | 0.11 | 0.48 | 0.29 | 0.68 |
| Dayal14, 1 $M_\odot$ yr$^{-1}$ | 0.36 | 0.64 | – | – |
| Dayal14, 5 $M_\odot$ yr$^{-1}$ | $6.9 \times 10^{-4}$ | $7.3 \times 10^{-4}$ | 2.8 | 1.4 |

Given the large uncertainty in the predicted galaxy luminosity function beyond $z \sim 10$, we investigated two theoretical predictions for the [CII] luminosity function with very different methodologies. The first method used star forming galaxy number counts of Chary & Pope (2010, CP10). These galaxy counts are based on backward-evolving

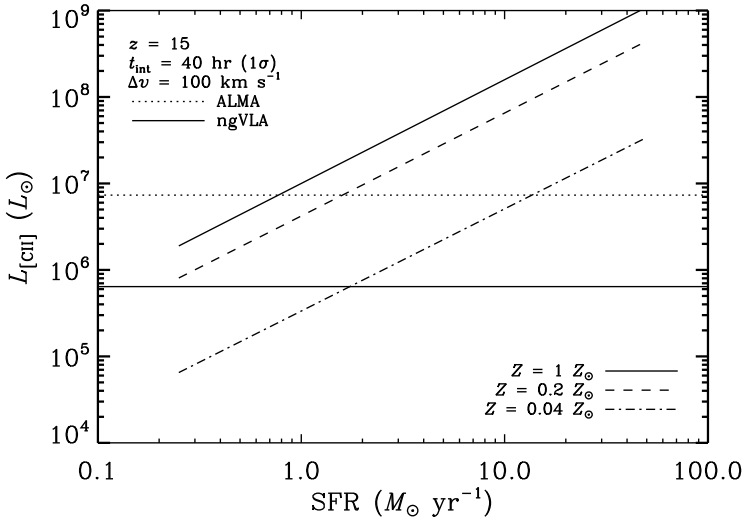


Figure 3. [CII] 158 $\mu$m line luminosity versus star formation rate and metallicity, based on the relationship given in Equation 12 of Vallini et al. (2015). Three different metallicities are shown. Also shown is the rms sensitivity of ALMA and the ngVLA for a galaxy at $z = 15$, assuming a 100 km s$^{-1}$ channel and 40 hr integration.

models for the infrared luminosity function of Chary & Elbaz (2001), anchored by a variety of observational data from *Spitzer* and *Herschel*.

The second method employed the calculations of high redshift galaxy formation of Dayal et al. (2014). This model aims at isolating the essential physics driving early galaxy formation via a merger-tree based semi-analytical model including the key physics of star formation, supernova feedback, and the growth of progressively more massive systems (via halo mergers and gas accretion). This model reproduces well both the slope and amplitude of the UV LF from $z = 5$ to $z = 10$.

The two models predict the cummulative co-moving number density of star-forming galaxies above a given star formation rate as a function of redshift. These values can be converted to cummulative number densities of [CII] emitting galaxies as a function of line flux, using the models of Vallini et al. (2015). The [CII] number densities vs. flux can then be turned into the number of observed galaxies in a given integration time, bandwidth, and field of view, using the sensitivities, field sizes, and bandwidths of the ngVLA and ALMA, as discussed in §3.

The ngVLA covers the 90 − 116 GHz range, corresponding to $z = 20$ to 15. We also consider just the number of galaxies between $z = 15$ and 16. ALMA has receivers that will cover from $z = 10$ to 15, or frequencies from 173 GHz to 116 GHz. Currently, the bandwidth is limited to 8 GHz. We consider an 8 GHz blind search in the Band 5 from 165 GHz to 173 GHz ($z = 10.5$ to 10), and one covering most of Band 4 with a hypothetical 32 GHz bandwidth system, from 126 GHz to 158 GHz ($z = 11$ to 14).

In Table 2, we tabulate the number of galaxies detected in [CII] emission per 40 hr integration per frequency tuning, for the ngVLA and ALMA, and for the different models. For the ngVLA, and for SFR $\geq 1\,M_\odot\,\mathrm{yr}^{-1}$, the models predict that one to two

independent pointings will be required to detect one galaxy over the full redshift range, on average. For the CP10 model, these sources have a broader redshift distribution, with 22% of the sources at $z = 15$ to 16. For the Dayal14 model, the majority (64%), of the sources are in this lowest redshift bin.

For ALMA and an SFR $\geq 5\,M_\odot\,\mathrm{yr}^{-1}$, the predicted number of detections differs significantly between models. For the 8 GHz bandwidth search in Band 5 ($z = 10$ to 10.5), the CP10 model requires about three pointings for a single detection, on average, while the Dayal14 model has more low redshift, brighter galaxies, with three sources per pointing expected. For the hypothetical 32 GHz bandwidth search in Band 4 ($z = 11$ to 14), the values are roughly two pointings needed for a single detection for the CP10 model, and one pointing needed for the Dayal14 model.

Overall, the detection rates in blind surveys will be slow (of order unity per 40 hr pointing). However, the observations are well suited to commensal searches on all programs employing the very wide bands that may be available in future.

A key issue in blind searches is spurious detections and verifying sources, especially given the large number of voxels searched for emission in the proposed surveys (see Carilli et al. 2017)). Recent blind line searches have developed some techniques for making statistical corrections to number counts based on e.g., comparing the number of negative and positive detections at a give level (Decarli et al. 2016; Walter et al. 2016; Aravena et al. 2016). However, the problem still remains as to how to verify that a given detection is associated with a $z > 10$ galaxy. One possible method will be broad band near-IR colors from e,g., *JWST*, or large ground based telescopes. Likewise, follow-up spectroscopy with large ground and space-based telescopes may reveal atomic lines (Barrow et al. 2017). Lastly, ALMA could be used to search for [OIII] 88$\mu$m emission, in cases of low metallicity galaxies (Cormier et al. 2015; Hashimoto et al. 2018a,b).

## 5. Conclusions

We have considered observing [CII] 158$\mu$m emission from $z = 10$ to 20 galaxies. The [CII] line may prove to be a powerful tool to determine spectroscopic redshifts, and galaxy dynamics, for the first galaxies at the end of the dark ages, such as identified as near-IR dropout candidates by *JWST*.

In 40 hr, the ngVLA has the sensitivity to detect the integrated [CII] line emission from moderate metallicity and (Milky-Way like) star formation rate galaxies ($Z_A = 0.2$, SFR = $1\,M_\odot\,\mathrm{yr}^{-1}$), at $z = 15$ at a significance of $6\sigma$. This significance reduces to $4\sigma$ at $z = 20$. In 40 hr, ALMA has the sensitivity to detect the integrated [CII] line emission from a higher star formation rate galaxy ($Z_A = 0.2\,Z_\odot$, SFR = $5\,M_\odot\,\mathrm{yr}^{-1}$), at $z = 10$ at a significance of $6\sigma$. This significance reduces to $4\sigma$ at $z = 15$. We also consider dependencies on metallically and star formation rate.

We perform imaging simulations using a plausible model for the gas dynamics of disk galaxies, scaled to the sizes and luminosities expected for these early galaxies. The ngVLA will recover rotation dynamics for active star-forming galaxies ($\gtrsim 5\,M_\odot\,\mathrm{yr}^{-1}$ at $z \sim 15$), in reasonable integration times.

We adopt two models for very high redshift galaxy formation, and calculate the expected detection rate for [CII] emission at $z \sim 10$ to 20, in blind, wide bandwidth, spectroscopic deep fields. The detection rates in blind surveys will be slow (of order

unity per 40 hr pointing). However, the observations are well suited to commensal searches on all programs employing the very wide bands that may be available in future.

**Acknowledgments.** PD acknowledges support from the European Research Council's starting grant ERC StG-717001 and from the European Commission's and University of Groningen's CO-FUND Rosalind Franklin program. The National Radio Astronomy Observatory is a facilites of the National Science Foundation operated under cooperative agreement by Associated Universities, Inc.. We thank Ranga-Ram Chary for discussions on the models and the paper, and N. Scoville for bringing up the possibility of very high $z$ [CII] in the ngVLA context.

**References**

Aravena, M.; Decarli, R.; Walter, F.; Bouwens, R.; Oesch, P. A. et al. 2016, ApJ, 833, 71
Barrow, Kirk S. S.; Wise, John H.; Norman, Michael L.; O'Shea, Brian W.; Xu, Hao 2017, MNRAS, 469, 4863
Carilli, C. L. & Shao, Y. 2017, Next Generation Very Large Array Memo No. 13 (http://library.nrao.edu/ngvla.shtml)
Carilli, C. L., & Walter, F. 2013, ARA&A, 51, 105
Carilli, C. L., Murphy, E., Ferrara, A., Dayal, P. 2017, ApJ, 848, 49
Chary, R.-R., & Pope, A. 2010, arXiv:1003.1731
Chary, R. & Elbaz, D. 2010, ApJ, 556, 562
Cormier, D., Madden, S. C., Lebouteiller, V., et al. 2015, A&A, 578, A53
Dayal, P., Ferrara, A., Dunlop, J. S., & Pacucci, F. 2014, MNRAS, 445, 2545
Decarli, Roberto; Walter, Fabian; Aravena, Manuel; Carilli, Chris; Bouwens, Rychard et al. 2016, ApJ, 833, 69
Duffy, A. R., Mutch, S. J., Poole, G. B., et al. 2017, arXiv:1705.07255
Helfer, T. T., Thornley, M. D., Regan, M. W., et al. 2003, ApJS, 145, 259
Hashimoto, T., Laporte, N., Mawatari, K. et al. et al. 2018, Nature, 557, 392
Hashimoto, T., Inoue, A., Mawatari, K. et al. et al. 2018, PASJ, submitted
Laporte, N., Ellis, R. S., Boone, F., et al. 2017, arXiv:1703.02039
Mashian, N., Oesch, P. A., & Loeb, A. 2016, MNRAS, 455, 2101
Selina, R. & Murphy, E. 2017, Next Generation Very Large Array Memo No. 17 (http://library.nrao.edu/ngvla.shtml)
Stacey, G. J., Geis, N., Genzel, R., et al. 1991, ApJ, 373, 423
Topping, M.W. & Shull, J.M. 2015, ApJ, 800, 97
Vallini, L., Gallerani, S., Ferrara, A., Pallottini, A., & Yue, B. 2015, ApJ, 813, 36
Velusamy, T., Langer, W. D., Goldsmith, P. F., & Pineda, J. L. 2015, A&A, 578, A135
Venemans, B. P., Walter, F., Decarli, R., Banados, E., Carilli, C. et al. 2017, ApJ, 851, 8
Walter, Fabian; Decarli, Roberto; Aravena, Manuel; Carilli, Chris; Bouwens, Rychard et al. 2016, ApJ, 833, 67
Yue, B., Ferrara, A., Pallottini, A., Gallerani, S., & Vallini, L. 2015, MNRAS, 450, 3829